Metals Materials And Processes, 2000, Vol. 12, No. 2 & 3, pp. 269 - 280.

RESIDUAL STRESSES AND THEIR MEASUREMENTS BY X-RAY DIFFRACTION METHODS

C.Balasingh and A.K.Singh*
**CSIR Emeritus Scientist,*
Materials Science Division, National Aerospace Laboratories, Bangalore 560 017, India.

(Received 10 January 2000)

Abstract : The residual stress plays a **key** role in determining the life and dimensional stability of a precision machine component. This article reviews the **various** factors leading to the formation of residual stresses and describes **the** x-ray diffraction technique for **the measurement** of **residual** stresses. Emphasis is given to the recent developments which. permit **the** estimation of (a) triaxial **stresses, (b)** stresses in the various phases of a multiphase material such **as** ceramic composites, **and** (c) the **stresses** in composites containing **non-crystalline** or poorly **crystalline materials such BE** polymer matrix **composites.** Some examples are given from the **work** carried **out** at the National **Aerospace** Laboratories.

Keywords: residual stress, measurement, X-ray diffraction

1. INTRODUCTION

The stresses that are present in a body in the absence of externally applied loads and body forces are termed as the residual stresses. Residual stresses can arise in almost every step of manufacturing process[1-4]. The main cause of residual stress formation is inhomogenous deformation. The processes involving high temperature[5] often lead to residual stresses as different regions cool at different rates causing inhomogenous deformation. Localised heating by the welding arc and the subsequent rapid cooling leads to the formation of residual stresses in weldments. The magnitude of residual stress in regions near the weld can be as high as the yield strength of the material being welded. In heat treatment of metals, if it is cooled rapidly, the surface and the interior contract at different rates. The surface regions, because of the temperature gradient, contract more than the interior. By the time the interior begins to cool, the outer regions are already rigid, resulting in compressive stresses at the surface balanced by tensile stresses in the interior. However, if the material undergoes phase transformation with volume changes, the state of stress gets altered. In some cases tensile residual stresses are observed.

Residual stresses are set up in composites when the matrix and the reinforcement have different coefficients of thermal expansion and the curing is done at elevated temperatures. For example in carbon fibre/epoxy laminates the thermal expansion coefficient of carbon in the fibre direction is $-1.8 \times 10^{-6}/^{\circ}C$ and that *of* epoxy $45 \times 10^{-6}/^{\circ}C$. The curing temperature is $170^{\circ}C$. Curing stresses in certain CFRP laminates may be large enough to cause ply failure in the absence of applied stress, or premature failure upon tensile loading. Al_2O_3/SiC ceramic whisker composite is a high temperature material with high strength and high stiffness. The thermal expansion coefficient of α-Al_2O_3 is $8.34 \times 10^{-6}/^{\circ}C$ and that of β-SiC $4.45 \times 10^{-6}/^{\circ}C$. Tensile stress is observed in the Al_2O_3 phase and very high compressive stress in the SiC fibre. In metal matrix composites also very high residual stresses are formed. The thermal residual stresses have a profound influence on the performance of the composite. The magnitude of stress depends on the processing parameters, volume percentage of the reinforcement and the surface treatment given to the composite. In finishing operations such as electrodeposition process also, occurrence of high residual stresses is observed[6]

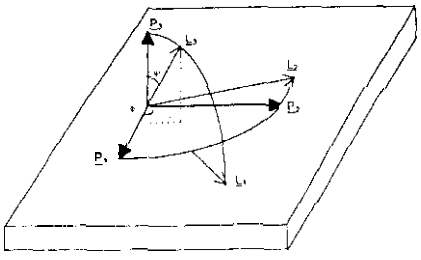

Fig.1 Definition of the angles ϕ and ψ and orientation of the laboratory system L_i with respect to the sample system P_i

Residual stresses can be beneficial as well as detrimental'? The service stresses are superimposed on residual stresses. Compressive surface residual stresses are desirable for they inhibit (i) initiation and propagation of fatigue crack and (ii) stress corrosion cracking. Many fabrication processes have been developed to exploit this phenomenon. Shot peening and other treatments are used to impart compressive stresses onto the surface of components. The deleterious effects of residual stress in a member are usually observed only after external loads or environmental effects are introduced, such that the combined effects cause noticeable damage. In the presence of residual stress, fatigue failures can be produced under external loads which by themselves would not have done so. Environments, which by themselves are not particularly damaging to a given material. cause failures in the presence of tensile residual stresses due to stress corrosion. The residual stresses in weldments cause distortion and other complex effects, most of which are undesirable. Castings with appreciable residual stresses are found to distort during storage, machining and service. High tensile residual stresses in electrodeposits lead to cracking, peeling and blistering of the deposits, and shrinkage and distortion of the articles plated.

2. STRESS MEASUREMENT BY X-RAY DIFFRACTION

X-ray diffraction was first applied to stress measurement in the year 1925. The early experiments used photographic method to record the diffraction pattern. Haskell[7] developed the elasticity equations in a form that could be applied to x-ray diffraction case. The principle of the method is discussed at length in books on x-ray diffraction [8-10]. When a beam of monochromatic x-rays fails on a polycrystalline material, diffraction occurs from those crystallites which are oriented to satisfy the Bragg's law

$$A = 2d\sin\theta \qquad (1)$$

where λ is the wavelength of the incident radiation,

d the interplanar spacing and

θ, the Bragg angle, is the angle the incident beam makes with the diffracting plane. In the case of a stress-free material, the interplanar spacing d, for a particular reflection (hkl), is constant from one crystallite to another. When it is deformed elastically, the lattice spacing of the crystallites change from their stress-free values, and cause a shift in the Bragg angle. The strain calculated from this shift is termed the lattice strain. The lattice strain will depend upon the orientation of the reflecting group of crystallites with respect to the direction of stress.

The effect of stress on x-ray diffraction can be conveniently discussed by considering two sets of orthogonal ca-ordinate systems shown in Fig.1. The axes P_i define the specimen with P_3 normal to the surface. It is required to measure stresses with respect to this co-ordinate system. The Laboratory system L_i is defined such that L_3 is in the direction of normal to the family of planes (hkl) whose spacing is measured by x-rays. L_2 is in the plane defined by P_3 and P_2 and makes an angle ϕ with P_2. The diffraction measurements are made in the L_j system. The two co-ordinate systems are oriented with respect to each

other by the angles ψ and ϕ. If the lattice spacing $d_{\phi\psi}$ is obtained from the measurement of the position of the diffraction peaks for a given (hkl), the strain along L_3 is given by

---

where d_o is the spacing of the planes in the stress-free state. In terms of the strains ε_{ij} the lattice strain can be written as

$$e_{\phi\psi} = \left[\varepsilon_{11}\cos^2\phi + \varepsilon_{12}\sin 2\phi + \varepsilon_{22}\sin^2\phi - \varepsilon_{33}\right]\sin^2\psi + \varepsilon_{33} + \left[\varepsilon_{13}\cos\phi + \varepsilon_{23}\sin\phi\right]\sin 2\psi \qquad (3)$$

This is the fundamental equation for x-ray stress determination. The stresses in the P_i co-ordinate system are given by

$$\sigma_{ij} = C_{ijkl}\,\varepsilon_{kl},$$

where the elastic stiffness coefficients C_{ijkl} are referred to the P_i system. If the material is isotropic, the stresses can be calculated using the relation

$$\sigma_{ij} = \frac{1}{\frac{1}{2}S_2}\left[\varepsilon_{ij} - \delta_{ij}\frac{S_1}{\frac{1}{2}S_2 + 3S_1}\left(\varepsilon_{11} + \varepsilon_{22} + \varepsilon_{33}\right)\right] \qquad (4)$$

where δ_{ij} is the Kronecker delta function,

$$\tfrac{1}{2}S_2 = (1+\nu)/E \quad and \quad S_1 = -\nu/E \qquad (5)$$

S_1 and $\frac{1}{2}S_2$ are referred to as X-ray Elastic Constants (XEC). The XEC are in general different from the bulk elastic constants .

Three interesting cases are observed from a closer examination of equation(3)

(a) If the shear components ε_{13} and ε_{23} are zero, the expression reduces to

$$e_{\phi\psi} = \left[E_{11}\cos^2\phi + E_{12}\sin 2\phi + \varepsilon_{22}\sin^2\phi - \varepsilon_{33}\right]\sin^2\psi + \varepsilon_{33} \qquad (6)$$

and we get a linear relationship between d and sin' ψ as shown in Fig.2a.

(b) When either or both shear components ε_{13}, ε_{23} are non zero, the interplanar spacing d measured at positive and negative ψ will be different due to the sin 2ψ term. This causes a split in the dversus $\sin^2\psi$ data, and this effect known as ψ splitting" is shown in Fig.2b.

(c) Equation (3) is derived on the assumption that the bulk material is elastically isotropic. This requires a random, orientation of the crystallites. However, the metal processing methods can develop texture. In such cases the d versus $\sin^2\psi$ plots exhibit an oscillatory behaviour (Fig. 2c). In case of steep stress gradients the d versus $\sin^2\psi$ plot is found to be slightly curved instead of a straight line.

The strains $\varepsilon_{\phi\psi}$ depend on the angles ϕ and ψ. Two choices are possible (i) the strains $\varepsilon_{\phi\psi}$ can be measured as a function of ψ for fixed values of ϕ. This is the conventional ψ-differential method. Depending on how ψ is changed there are two techniques called the iso-inclination method and the side inclination method. (ii) the strains $\varepsilon_{\phi\psi}$ are

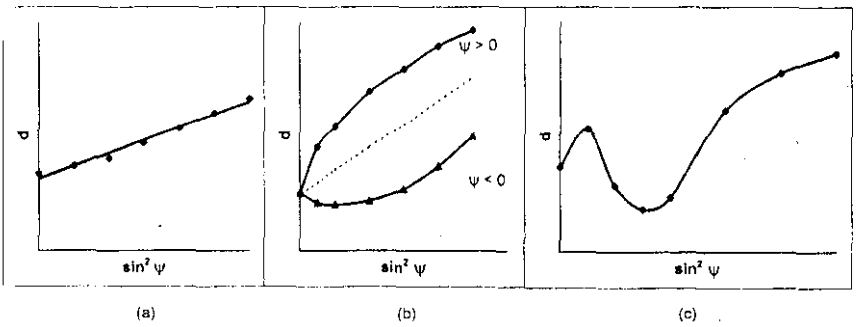

Fig 2 Types of d vs $\sin^2\psi$ plot commonly encountered In residual **stress analysis**

measured as a function of ϕ for fixed values of ψ . This is called the phi-integral method[""]. Any one of these techniques can be followed, and strains and stresses determined.

In most of the cases, especially in metals, the penetration depth is small. And if steep stress gradients are not present, the equations for stress measurement can be simplified by assuming a biaxial state of stress, the stress normal to the free surface being zero. The d-spacings are measured for different ψ values and the stress calculated using the relation

$$\sigma_\phi = \frac{E}{1+\nu}\frac{1}{\sin^2\psi}\frac{d_\psi - d_\perp}{d_0}$$

For practical purposes, d_0 in the denominator can be replaced by $d_\perp$ without introducing much error. Here, $d_\perp$ refers to the d-spacing with ψ=0 . The quantity

$$\frac{d_\psi - d_\perp}{d_\perp}\frac{1}{\sin^2\psi}$$

is determined by a least square procedure by measurement at different ψ values. In case the penetration depth is high, as in case of ceramic composites, or if steep stress gradients are present, the equations pertaining to the generalised 3-dimensional case of stress are to be used. ε_{ij} are calculated by determining $e_{\phi\psi}$ at ϕ = 0, 90 and 45^0. At each ϕ ,measurements are to be done at both positive and negative ψ values [11,13]. ε_{ij} are converted into stresses using equation(4).

2.1 Stresses in multiphase systems

One of the major advantages of XRD method is its ability to measure stresses in individual phases of a multiphase material. Macrostresses arise from differences in processing from one macroscopic region to another e.g.: between surface layer and interior as a result of cutting, grinding, temperature gradients during cooling etc. They are defined to be the same in each phase (the mechanical methods detect only this type of stresses). Microstresses arise from microscopic constraints between the phases, caused for example, by differences in thermal expansion and elastic constraints, and bonding

between the phases. Consider a two phase composite processed at high temperature. At the processing temperature the contact boundaries between the two phase particles are bond well, and on cooling to room temperature the bulk material contracts. If the two phases have different coefficients of thermal expansion, they try to contract by different amounts. A good bonding on the contact surfaces of the two-phase particles imposes constraint on free contraction. The phase with larger coefficient of thermal expansion is left in tension, while compressive stress in particles of phase with a lower thermal expansion provides the force balance. The actual magnitude of stress in individual particle will depend on its orientation with respect to the neighbouring particles since the particles in general have anisotropic thermal and elastic properties. Thus if a large enough volume compared to the size of the particles is considered, phase **1** will have a mean tensile stress which will cause a shift, and a broadening of the diffraction peak. Similarly phase 2 will have a mean compressional stress. It may be noted that stress in any direction in the bulk sample is zero. Thus, we have a very special case where the stress in the two phases cause peak shifl in the absence of a resultant stress in the bulk material. For this reason, these stresses are called pseudo-macrostresses (p-m stresses)[4].

Methods have been developed to separate the macrostresses from p-m stresses. The stresses obtained from the shifl in XRD lines contains contributions from macro, pseudo-macro as well as applied stresses. The contributions from the macro and p-m stresses may be identified by considering the conditions of equilibrium. The average stress obtained from any phase can be written as

$$\langle \sigma_{ij} \rangle^{k} = \sigma_{ij}^{m} + \langle \sigma_{ij} \rangle^{\mu,k}$$

where $k=\alpha, \beta$, for a two-phase material. σ_{ij}^{m} is the macrostresses and $\langle \sigma_{ij} \rangle^{\mu,k}$ the p-m stress in the k^{th} phase. Macrostresses σ_{ij}^{m} must satisfy the usual conditions of equilibrium. These equations along with a knowledge of the volume fraction of the phases are used to separate out the macro and p-m stresses.

3. EQUIPMENT

In the initial stages, stress measurements were carried out by the photographic method using back reflection cameras. Slowly the emphasis shifted to diffractometer as it is faster and gives higher precision on measurements. However, the photographic method has still some advantages . The method is simple and is comparatively less expensive. Further, beam size can be alfered and .point to point measurement possible. Recent advances in photosensitive microchips 'and photodiode arrays are slowly replacing the x-ray films. These solid state cameras combine the desirable features of the traditional film camera and diffractometer techniques. For stress analysis usually two photodiode arrays are positioned symmetrically around the collimator in analogy to the conventional back reflection film technique[14]. Data acquisition and processing are done by microcomputers, With this set-up measurements can be done rapidly, individual exposures being a few seconds and stress in any particular direction being determined within a minute.

The conventional diffractometers can be used to measure stresses. But the size of the sample which can be examined is limited. To measure residual stresses in large components or assemblies, mobile stress diffractometers are to be used. They are commercially available.

3.1 Factors affecting precision

A few factors affect the precision of x-ray stress measurement, and one should be aware of them while using the technique. One relatively major and sometimes troublesome

problem is the positioning of the specimen surface along the axis of the goniometer. This may prove to be rather difficult when the geometry of the specimen is complicated. The errors can be theoretically calculated[15,16] and corrected or experimentally corrected by using a thin layer of calibrating substance on the surface of the specimen. Parallel beam geometry is employed to reduce the sensitivity of displacement error on sample position. But the sharpness of the diffraction peak is lost leading to less precise estimate of the peak position, The θ- dependent factors which affect the diffracted intensity are Lorentz polarisation and absorption factors. These corrections need be applied only in case of broad lines. Another source of error is the use of elastic constants. The intensity entering the detector arises only from the crystaliites that are suitably oriented. Naturally the use of E and ν obtained from mechanical testing can lead to errors, serious in certain cases. X-ray elastic constants can be theoretically calculated or experimentally determined. In case of textured materials, the non linearity in d versus $\sin^2\psi$ makes the calculation of stress difficult. Different methods have been suggested for the calculation of stresses[17-19] in such cases.

3.2. Surface preparation

Since the penetrating power of x-rays used for diffraction is small, the surface preparation is very important. If there are pits the stress value determined by x-rays may not be the true stress. The surface should be smooth. This can be achieved by surface grinding followed by mechanical polishing. The disturbed layer should be removed by electropolishing. However, the surface should not be touched at all prior to stress measurement if the aim is to measure residual stresses caused by treatment such as machining, grinding, shot peening etc.

3.3 Limitation

The main limitation of the method is that it can be used only for the evaluation of surface residual stresses. If stress distribution through the thickness is required the surface layers have to be removed by electropolishing . For non-destructive depth profiling of residual stresses, neutron diffraction is the best method. The neutron diffraction method has been successfully used in profiling of residual stress gradients in heat treated, joined or formed metallic, ceramic or composite materials; determination of triaxial stress tensors and gradients in the interior of solid material: and stress concentrations around holes, notches etc. Though the method has many advantages, it is not very popular as it is costly, and neutron sources are available only in a few places.

4. SOME EXAMPLES

A few cases are presented to illustrate the capabilities of XRD technique in the measurement of residual stresses in different types of components and materials.

4.1 Residual stresses in artificial heart valve cages[20]

The mechanical heart valve consists of three parts: an occluder, a cage made of metal to house the occluder and sewing ring. The cage is machined from a solid block of Haynes 25 cobalt base superalloy. The cage has ring section (Fig. 3) and three struts. Two of these struts are longer than the third one, and are referred to as major struts. The critical locations were identified as the places where the major struts join the ring section and hence residual stress evaluations at these locations became necessary. The area over

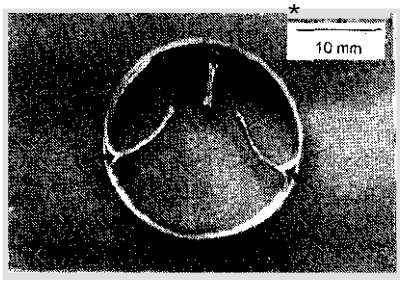

Fig 3 The heart-valve cage Stress measurements *were* made at the locations indicated by the *arrows*

which residual stress measurements were to be done is about 1 mm diameter. The cage was mounted on the diffractometer such that the area of interest was along the axis and only that portion was illuminated by the incident beam. This was achieved by using a smaller divergent slit and use of lead pieces to cut down the axial dimension. . The ψ differential method was followed, the diffraction peak positions being determined by the profile fitting procedure. The residual stress value was found to be 136 MPa tensile, which was too high for acceptance. The machining procedure was changed in the second cage which gave a stress value of +70 MPa.

4.2 Residual stresses in ceramic composites

The next example is a ceramic composite: ***a-*** Al_2O_3/ β–SiC (whisker). The incorporation of β-SiC whiskers into α-Al_2O_3 produces significant increase in mechanical strength and fracture toughness. Residual stresses play a direct role in some of the failure processes, particularly whisker pull out, frictional bonding and the incidence of microcracking. The composites are hot pressed and the difference in thermal expansion coefficients causes formation of residual stresses. Residual strains in both the phases were measured by the XRD method and macro and p-m stresses separated out. The (146) reflection from alumina and (511,333) reflection from silicon carbide were found suitable for stress measurement and the profiles overlapped partially (Fig.4). Peak positions were determined using profile fitting program. The graphical and the generalised least squares procedures were used to compute the, triaxial strain/stress components from the measured lattice strains. The strains and stresses in a sample with 29 vol. % of SiC are given in Table I. The shear components were almost zero and hence neglected. The macrostresses are tensile and low in magnitude, whereas p-m stresses are quite high in magnitude (compressive in the whiskers'and tensile in the matrix) and nearly hydrostatic. In this case the macrostresses are due to the grinding operation, whereas the p-m stresses are due to the difference in thermal expansion coefficients.

4.3 Residual stresses in Al alloy sheet/ Ararnid fibre laminated composites

Al alloy/ Kevlar-epoxy laminates, popularly known as ARALL, have many attractive properties like higher strength to weight ratio, higher UTS and fatigue properties compared *to* monolithic aluminium sheets. During fabrication, the laminates are subjected to a temperature of 120^0C or higher. Since the aramid fibres have a negative coefficient of thermal expansion in the fibre direction, the as-prepared laminates have aluminium layers in tension . As tensile residual stresses affect the fatigue properties the laminates are often'prestrained to produce compressive residual stresses in aluminium layers.

Arall consisting of three layers of L59 Al alloy and two layers of Kevlar epoxy composite were prepared and residual stresses in Al sheets measured by the XRD and strain gauge techniques. The x-ray measurements were made with a diffractometer using copper radiation and the high angle (511,333) reflection of Al. On each specimen, stresses were measured both parallel and perpendicular *to* the fibre direction. Residual stress in the Al alloy in the fibre direction was tensile and that in the perpendicular direction compressive. The magnitude of stresses varied from batch to batch, probably due to variation in the

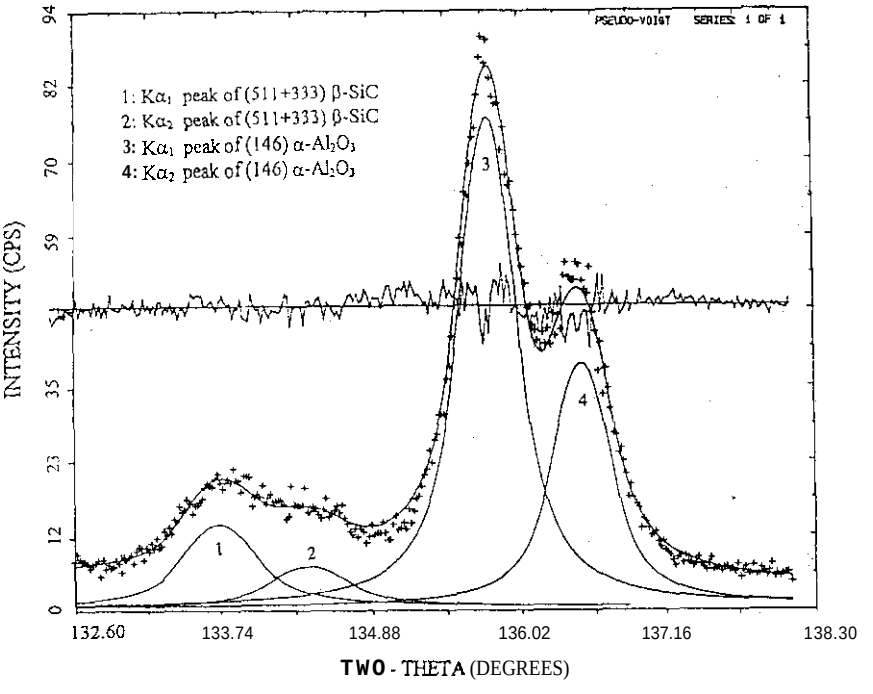

Fig. 4. Diffraction pattern of a ceramic composile specimen from 132.6^0 to 138.3^0 2 θ showing raw data (crosses), profile fit to a pseudo-Voigt function showing the individual peaks with background subtracted (solid lines). the sum of the individual peaks plus background (solid lines through raw data), and the difference between the fit and the raw data (horizontal trace).

Table Ia. Total residual strains in a composite specimen

	(146)	SIC (511, 333)
ε_{11} (in 10^{-6})	656	-1405
ε_{22} (in 10^{-6})	733	-1349
ε_{33} (in 10^{-6})	433	-1680

Table Ib. Macro and p-m stresses

	Macrostresses (MPa)	.p-m stresses (MPa)	
		Al_2O_3	SiC
σ_{11}	79	395	-957
σ_{22}	102	397	-961
σ_{33}	0	400	-956

resin-fibre ratio from batch to batch. The stress determined. by the two techniques agree quite well. The maximum residual stress observed was 33 MPa.

4.4 Residual stress distribution in shot peened AlLi alloy sheets[23]

AlLi alloys are potential aircraft materials because of their light weight, high strength to weight ratio, good surface finishing, good corrosion resistance and reflectivity. It also exhibits good low temperature properties. A systematic study was undertaken to measure residual stress distribution in shot peened Lital A AlLi alloy sheets of thickness 7.89 mm. The residual stress measurements were carried out by the XRD method. To determine the stress distribution across the thickness, known thickness of the material is removed from the surface *of* the specimen by electropolishing technique. The temperature of the electrolyte and the potential between the electrodes were adjusted to achieve uniform layer removal without pitting. In shot peened components, the magnitude 'of residual

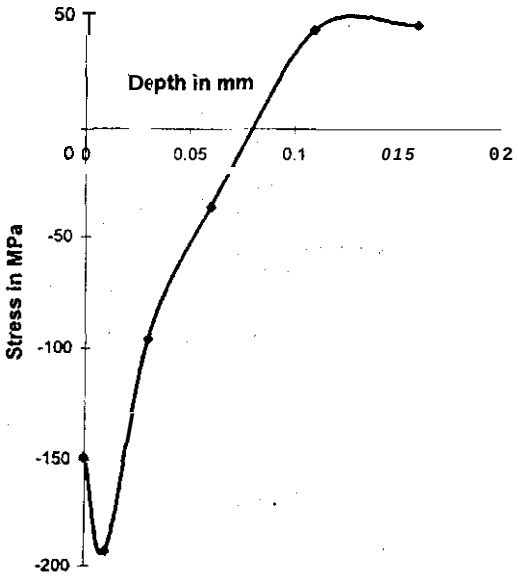

Fig. 5. Residual stress distribution in in Lital A sheet peened with glass beads

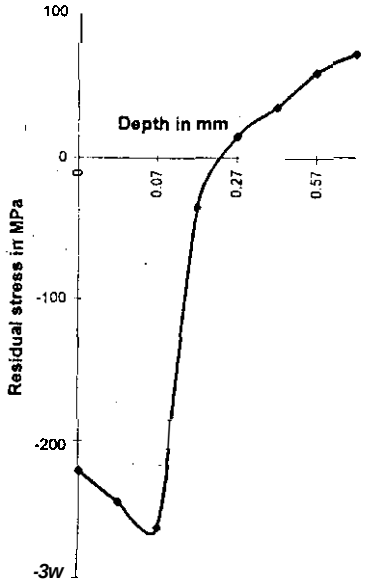

Fig. 6. Residual stress distribution in in Lital A sheet peened with steel shots

stress induced depends on peening parameters such as shot size, shot velocity etc. Lital A sheets were subjected to shot peening using steel shots and glass beads. Shot peening was done normal to the surface at a pressure of 30 psi. These peening conditions gave an intensity of 8 thou Almen arc height for peening with steel shots and 6 thou for peening with glass beads.

The residual stress distribution in the Lital A sheets peened with glass beads and steel shots are given in Figures 5 and 6 respectively. For comparison residual stress distribution in the as-received Lital A sheet is given in Fig. 7. It is seen that in all cases the stress at the surface is compressive. In the as-received sample the magnitude of stresses in the rolling and trahsverse direction are different. In the as-received sheet the maximum compressive stress is observed at the surface. But in shot peened specimens the maximum compressive stress is not observed at the surface, but at a depth below the surface. Further it can be observed that (i) the maximum compressive stress is larger for the sample peened with steel shots compared to that peened with glass beads. (ii) the depth at which the maximum compressive stress occurs is greater for the sample peened with steel shots. These can be understood and explained in terms of the kinetic energy imparted by the shots to the sample.

4.5 Residual stress in First stage Turbine wheels

To salvage the Turbine wheels taken from the accident engines, residual stress measurements were carried out on wheels (Fig. 8) removed from an overhauled engine and that removed from accident engine. The XRD measurements were done using a General Electric Goniometer. The x-ray diffraction profile was found to be broad with low peak to baokground ratio. This necessitated large counting time to reduce statistical errors. The peak positions were determined by profile fitting technique. The Lorentzian function was found to give the best fit of the observed profile. The measurements were done at a number of critical locations in both the wheels. Residual stresses in both the

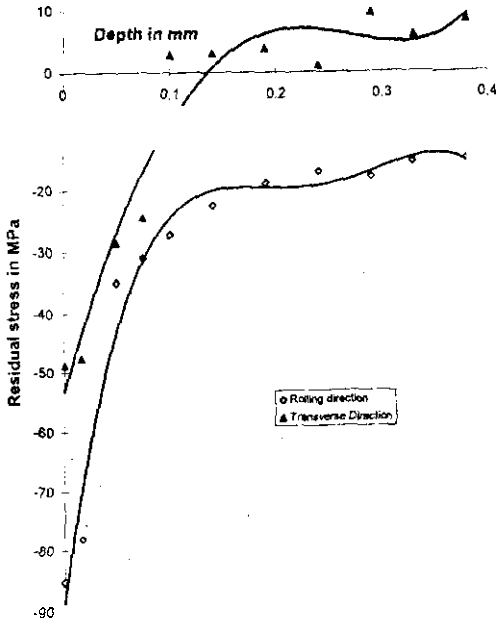

Fig. 7. **Residual stress** distribution in the **as-received** Lital A sheet

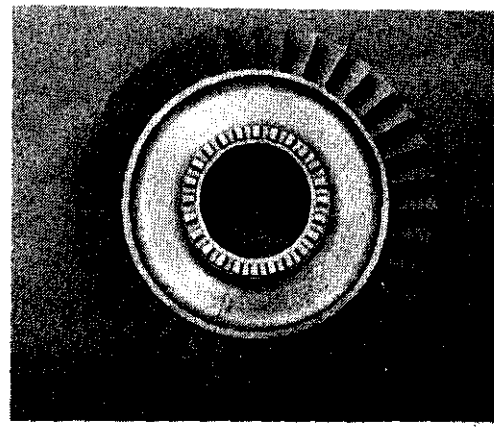

Fig. **8** . *Turbine* **wheel**

discs were found to be compressive in nature and the magnitude same within experimental errors.

4.6 Stresses **in CFRP** laminates[24]

Residual stresses in laminates are of two types (i) microstresses or p-m stresses in each ply of the constituent phase within a given ply. These stresses arise because of the difference in thermal and moisture expansion between the phases. (ii) macrostresses in each ply, considered to be homogeneous, having anisotropic thermal and moisture expansion. These stresses arise because of the constraints by the neighbouring plies. The XRD technique cannot be directly used to measure stresses in polymer composites because the phases present do not give strong diffraction pattern. But it is possible to measure residual stresses in these systems, if small amounts of particles with suitable diffracting characteristics are incorporated into the composite. The strains and stresses in these particles are measured by the XRD method and a calibration procedure adopted to relate these strains to the strains and stresses in the composite.

Unidirectional CFRP laminates were made by stacking seven layers of prepregs. While laying up, on the sixth layer, a very fine layer of Al powder was sprinkled. The thickness of the laminate was 1.1 mm. From these laminates specimens were cut for tensile testing, calibration and residual stress measurement. Calibration was done by applying known loads to the composite and measuring the position of the XRD lines from the Al particles. Loads were applied to produce strains in steps of 100 or 200×10^{-6} and the corresponding strains from the Al particles measured at different inclination angles. For the determination of residual stresses, coupons of 4 cm x 4 cm were cut. X-ray measurements were done at different azimuth and inclination angles. The composite residual strain is found by replotting the particle strain as a function of composite strain and doing a bit of extrapolation. This procedure gave a matrix p-m stress of '18 MPa. Theoretical calculations based on the differential coefficient of thermal expansion gives a matrix stress of 25 MPa in the fibre direction. The experimentally obtained value is close (but not equal) to the theoretical value. Calculation of residual stress in these systems by a finite method gives a matrix stress of 26 Mpa. The discrepancy can be qualitatively attributed to: (a) many particles are present in the 1,2 plane and quite likely the development of full

residual stress is inhibited. (b) also the particle strains perpendicular to the fibre direction are not equal, which should have been the case if the matrix is unaffected by the crystalline particles. It is to be noted that unidirectional laminates containing no filler particles are transversely isotropic. The experimental measurements can, in principle, be improved by using fewer crystalline particles. But the use of fewer particles is beset with practical difficulties.'Although the measured values do differ slightly from the theoretical value, the XRD technique can be very effectively used to monitor the variation in composite strain caused by factors like moisture absorption.

5. CONCLUSION

X-ray diffraction provides a powerful technique for the evaluation of residual stresses. The method has been successfully used in a wide variety of cases. The x-ray diffraction method is applicable to crystalline materials like metals and ceramics. However, now the method can be applied to noncrystalline composite materials also by the introduction of an extremely thin layer of crystalline material during the fabrication. The ability of the method to measure stresses in the individual phases of a multiphase material is a major advantage of the technique.

REFERENCES

1. E. Kula and V. Weiss, Residual Stress and Stress Relaxation, Plenum Press, 1982
2. Larry J.Vande Walle, Residual Stress for Designers and Metallurgists, HSM, Ohio, 1981
3. W B Young, Residual Stress in Design, Process and Materials Selection, ASM, Ohio, 1987
4. I. C. Noyan, and J. B. Cohen, Residual Stress: Measurement by x-ray diffraction and Interpretation, Springer Verlag 1987
5. Balasingh. C., Seshadri, M. R., Ramaseshan, S. and Srinivasa, M. N., J. of Ind. Inst of Science, 1977, **59**(9), 323.
6. Subramanian, R., Balasingh, C. and Shenoi, B. A., Metal Finishing, 1967, **65,** 67.
7. R.K.Haskell, X-ray diffraction as applied to the determination of stress conditions in gun metals, Watertown Arsenal Report No.160/2, Watertown, MA
8. B.D.Cullity, Elements of X-ray diffraction, Addison-Wesley Publishing Co., 1978
9. A.Taylor, X-ray Metallography, John Wiley & Sons, 1961
10. C.S.Barrett and T.B.Massalski, Structure of Metals, Pergamon Press, 1980
11. Dolle. H., J. Appl. Cryst., 1979, **12,** 489.
12. Wagner, C. N. J., Eigenmann, B. and Boldrick, M. S., Adv. In X-ray Analysis, 1988, 31, 181.
13. Dolle, H. and Cohen, J. B., Metall. Trans., 1980, **11A**, 159.
14. Korhonen, M. A., Lindroos, V. K. and Suominen, L. S., Adv. in X-ray Analysis, 1989, **32,** 407.
15. Singh, A. K. and Balasingh, C., J.Appl.Phys., 1971, **42(13)**, 5254.

16. Singh. A. K. and Balasingh, C.. J.Appl.Cryst., 1973,6,466.

17. Peyer R.Morris, Int. J. Engng. Sci., 1970,8, 49.

18. Brakman, C. M., J. Appl. Cryst.. 1989,20,479.

19. Penning, P. and Brakman, C. M., Acta Cryst., 1988,A44, 157.

20. C.Balasingh, S.Usha Devi and A.K.Singh, Measurement of Residual stresses in artificial heart valve cages, Report NAL PDMT9216, (1992)

21. Abuhasan, A., Balasingh, C. and Predecki, P., J. Am. Ceram. Soc., 1990,73(8), 2474.

22. Balasingh. C., Kanakalatha, P., Sridhar, M. K. and Singh, A. K.. Ind.J.Phys., 1989, 63A, 262.

23. K. Mangala, Residual stress distribution in shot peened AlLi alloy, ME Thesis, REC Thiruchirappalli 1991

24. Balasingh, C. and Vandana Singh, Bull. of Mater. Sci., 1997,20(3), 325.